Biochemical and Biophysical Research Communications 421 (2012) 361–366

Contents lists available at SciVerse ScienceDirect

Biochemical and Biophysical Research Communications

journal homepage: www.elsevier.com/locate/ybbrc

Live free or die: Stretch-induced apoptosis occurs when adaptive reorientation of annulus fibrosus cells is restricted

Rosalyn D. Abbott [a], Alan K. Howe [b], Helene M. Langevin [c], James C. Iatridis [d,*]

[a] School of Engineering, University of Vermont, Burlington, VT 05405, USA
[b] Department of Pharmacology, University of Vermont, Burlington, VT 05405, USA
[c] Department of Neurology, University of Vermont, Burlington, VT 05405, USA
[d] Department of Orthopaedics, Mount Sinai School of Medicine, NY 10029, USA

ARTICLE INFO

Article history:
Received 31 March 2012
Available online 9 April 2012

Keywords:
Intervertebral disc
Annulus fibrosus
Cyclic tensile stretch
Cytoskeleton
Actin filaments
Apoptosis
Caspase-3

ABSTRACT

High matrix strains in the intervertebral disc occur during physiological motions and are amplified around structural defects in the annulus fibrosus (AF). It remains unknown if large matrix strains in the human AF result in localized cell death. This study investigated strain amplitudes and substrate conditions where AF cells were vulnerable to stretch-induced apoptosis. Human degenerated AF cells were subjected to 1 Hz-cyclic tensile strains for 24 h on uniformly collagen coated substrates and on substrates with 40 μm stripes of collagen that restricted cellular reorientation. AF cells were capable of responding to stretch (stress fibers and focal adhesions aligned perpendicular to the direction of stretch), but were vulnerable to stretch-induced apoptosis when cytoskeletal reorientation was restricted, as could occur in degenerated states due to fibrosis and crosslink accumulation and at areas where high strains occur (around structural defects, delaminations, and herniations).

1. Introduction

The loss of cellularity in human intervertebral disc (IVD) degeneration is generally associated with reduced glucose and accumulation of lactic acid due to anaerobic metabolism and limited waste removal in IVDs with calcified endplates [1,2]. However, some cell death likely occurs due to structural changes in the matrix [3,4] that affect the cell microenvironment. Matrix strains are concentrated adjacent to large defects, such as clefts, fissures, and herniations that occur with degeneration [5,6], near nucleotomy sites [7], as well as near small defects such as needle puncture injuries [8]. Notably cell death is also known to occur adjacent to injury sites, as near needle puncture injuries in the IVDs [9]. In this study, we explore the concept that some of the reduced cellularity in the IVD with degeneration is associated with stretch-induced apoptosis caused by high strain environments that occur due to structural changes and defects.

Under healthy conditions AF surface strains up to 6% were measured along the fiber direction [10] and AF fiber strains were calculated to be ~15% with a structural model [11]. AF strains calculated from MRI support the presence of large axial, radial and shear strains under physiological loading and further demonstrate strain amplification during injury and degeneration [5,7]. High magnitudes of cyclic equibiaxial strain induced apoptosis at 15% stretch in rabbit AF cells [12] and at 20% stretch in rat AF cells [13,14], however equibiaxial strain suppresses reorientation effects observed in pure uniaxial stretch of other cell types [15–17]. The hypothesis of this study was that human degenerated AF cells obtained from surgical samples reorient perpendicular to excessive uniaxial strains (10%, 15%, and 20% stretch), as observed in other cell types, but will undergo apoptosis when their adaptive reorientation is restricted as might occur around defects or crosslinking found with degeneration.

2. Materials and methods

2.1. Isolation and culture of human AF cells from surgical samples

AF tissue was obtained from patients undergoing anterior interbody fusions for low back pain secondary to degenerative disc disease with institutional review board approval and graded by the surgeon as either grade 4 ($n = 2$) or grade 5 ($n = 2$) on the Thompson scale [18]. Cells were released from surgical tissue by sequential enzymatic digestion (0.2% protease, 0.2% collagenase, Sigma–Aldrich, St. Louis, MO). Isolated cells were filtered (70 μm mesh, Thermo Fisher Scientific, Pittsburgh, PA), washed twice with PBS, then expanded in culture in high glucose DMEM (Invitrogen

* Corresponding author. Address: Mount Sinai School of Medicine, Leni and Peter W. May Department of Orthopaedics, One Gustave L. Levy Place, Box 1188, NY 10029-6574, USA. Fax: +1 212 876 3168.
E-mail addresses: Rosalyn.Abbott@uvm.edu (R.D. Abbott), james.iatridis@mssm.edu (J.C. Iatridis).

0006-291X/$ - see front matter © 2012 Elsevier Inc. All rights reserved.
http://dx.doi.org/10.1016/j.bbrc.2012.04.018

Lifesciences–Gibco, Carlsbad, CA), containing 10% fetal bovine serum (Atlanta Biologicals, Lawrenceville, GA), 1% penicillin/streptomycin (Gibco), 0.5% fungizone (Gibco), and 50 μg/mL ascorbate (Sigma–Aldrich). All experiments were performed on passage II or III cells.

2.2. Experiments on a uniform collagen coated surface

Cells were seeded at a density of 100,000 cells/cm^2 in precoated silicone elastic membranes (4 cm^2 molds from STREX, www.b-bridge.com, coated with type I bovine collagen, Sigma–Aldrich C4361, 40 μg/mL in PBS, overnight at 4 °C). The cells were cultured in hypoxic conditions (5% O_2) for 24 h to allow for attachment. Cells were assigned to either an unstretched control group (placed in the same incubator for 24 h), or stretched 10%, 15%, or 20% on a uniaxial cell stretch device (STREX) loaded at 1 Hz for 24 h in hypoxic conditions. Control and stretched cells were imaged following loading, the supernatant was saved, and the remaining cells were either trypsinized (Gibco, no EDTA) for flow cytometry to evaluate stretch-induced apoptosis, lysed (Qiagen, Valencia, CA) for qRT-PCR, or fixed with 10% formalin (Fisher) for immunohistochemistry to evaluate reorientation effects.

For flow cytometry, the supernatant was centrifuged to obtain detached cells. Ethanol induced apoptotic positive controls cells were always used to set up compensations and quadrants. Detached cells, attached cells, and apoptotic controls were washed twice with cold PBS and were resuspended in 100 μl of 1× Binding Buffer (BD Biosciences, San Diego, CA). They were stained with 10 μl of a 50 μg/ml stock of propidium iodine and 5 μl of FITC annexin V (Annexin V-FITC apoptosis detection kit I, BD Bioscience), and were added to TRU count tubes (BD Bioscience). The tubes were gently vortexed and incubated for 15 min at 25 °C in the dark. 400 μl of 1× Binding Buffer was then added to each tube and analyzed by flow cytometry within 1 h. Phosphatidylserine is externalized in apoptosis [19], therefore, Annexin V staining of phosphatidylserine on propidium iodide (PI) negative cells was used to quantitate apoptosis. Dual staining of Annexin V and PI identified late stage apoptotic or necrotic cells, as both dyes are membrane impermeable and can only enter and stain cells with compromised membrane integrity. PI staining in the absence of annexin V staining identifies necrotic material. Absolute numbers of cells were calculated for detached and attached conditions, and results were expressed as percentage difference from control.

For qRT-PCR, RNA was isolated from the lysed cells, cDNA synthesized, and nine genes were investigated: Caspase-3, Collagen types I and II, Elastin, MMP1, Proliferating Cell Nuclear Antigen (PCNA), Aggrecan, and SOX9 (Taqman, Applied Biosystems, Bedford, MA). Relative gene expression was calculated using the comparative Ct method normalized to cells in the control group and 18S.

For immunohistochemistry, cells were stained with a primary antibody against paxillin (BD Bioscience, Clone 349, 1/500) and an Alexa 594-conjugated secondary antibody (Invitrogen, 1/500) to indicate attachment to the ECM through focal adhesions. Cells were counterstained with DAPI (Invitrogen, 1:1000) and Alexa 488-phalloidin (Invitrogen, 1/100) to visualize the nucleus and F-actin, respectively.

The 2D discrete Fourier transform (DFT) was used to calculate orientation distributions of control and stretched cells [20] using a custom Matlab script. An autocorrelation function was used to determine if there was non-randomness in the resulting Fourier transform. It was determined that all three stretch conditions displayed a Gaussian distribution, while the control cells were random. A Gaussian distribution was then fit to the stretch data using a least square routine to characterize symmetric distributions [21]. The mean of the distribution was used to characterize the maximum angle of alignment within an image, while the standard deviation was used as an index to characterize the overall variance within an image.

2.3. Experiments with micropatterned collagen to restrict reorientation adaptation

A technique akin to micromolding in capillaries [22] was used to coat stripes of collagen type I to restrict the adaptive reorientation mechanism of the cells in response to high strains (Fig. 1). A master mold was created using standard soft lithography techniques [22]. Briefly, a photomask was created with AutoCad (width of features = 40 μm, length = 20 mm, Autodesk, San Rafael, CA) and printed (Advance Reproductions Corporation, North Andover, MA). A silicon wafer was spin coated with a uniform, 50–80 μm thick layer of SU-8 2035 negative photoresist (MicroChem, Newton, MA). The photoresist was exposed to ultraviolet light through the photomask to create a positive relief of the pattern using the following protocol: soft bake at 75 °C for 2 min and 105 °C for 7 min, expose for 15 s 100% power (IntelliRay 400, UviTron) and post exposure bake at 75 °C for 1 min and 105 °C for 5 min.

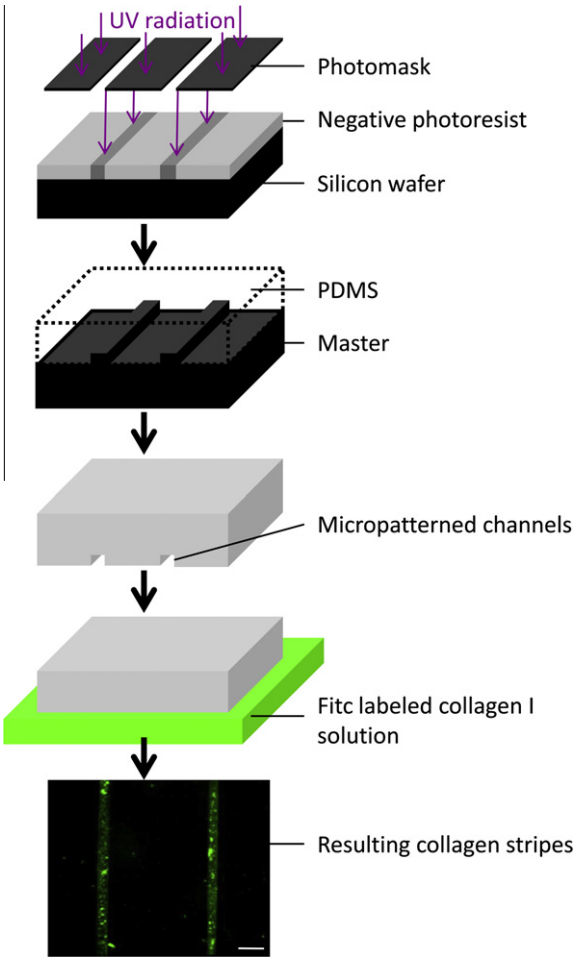

Fig. 1. Fabrication of 40 μm collagen stripes to restrict cellular reorientation. A silicon wafer was spin coated with a uniform layer of negative photoresist. UV radiation and a photomask was used to selectively expose the photoresist. Areas that were not exposed to the UV radiation become soluble in developer leaving only the desired pattern. PDMS was then cast against the photoresist master to create a relief of the 3D topography. The PDMS containing the microchannel features was then brought in contact with the silicone elastic substrate. A fitc labeled collagen type I solution submerged the PDMS overnight, confirming the collagen stripe pattern (scale bar = 100 μm).

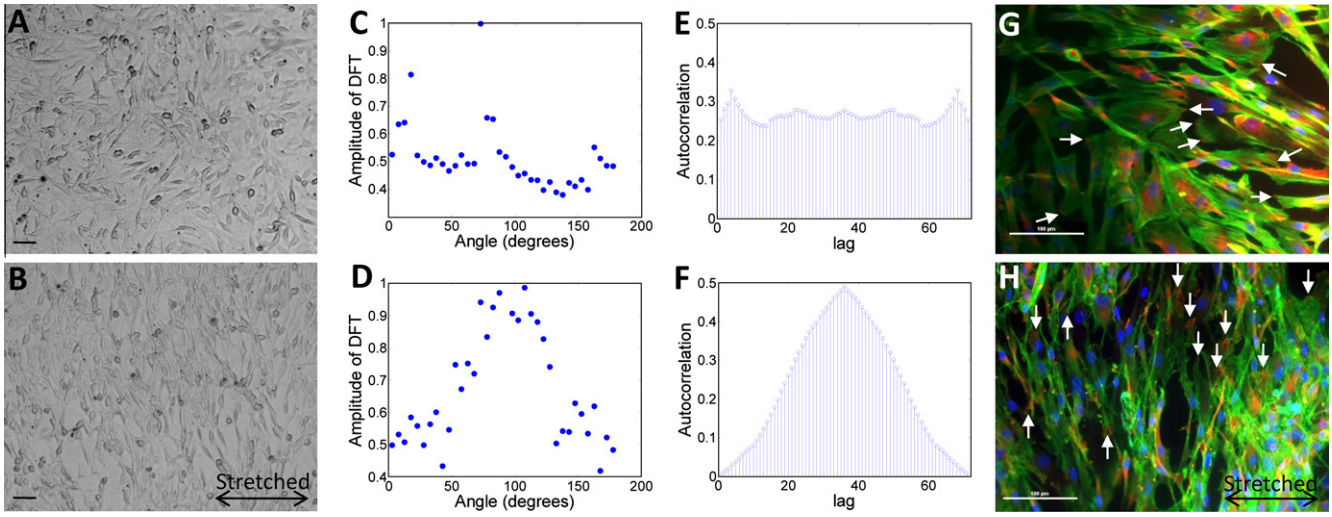

Fig. 2. Cytoskeletal remodeling in response to stretch involved reorientation perpendicular to the direction of stretch (90°) through the redistribution of actin and focal adhesions. The discrete fourier transform (DFT) was used to quantitate angular distribution of cells. Representative images of unstretched (A) and 20% stretched (B) cells with the corresponding DFT (C and D, respectively), where the location of peaks in the amplitude corresponds to preferential orientation of cells in that direction. Autocorrelation demonstrated that control images were random (E) while the stretch groups displayed a Gaussian pattern (F). Gaussian curves were fit to the DFT of stretched cells with the mean indicating angle of alignment, and standard deviation the amount of variance within an image. Cellular orientation was clear on imaging of control (G) and stretched (H) cells stained with DAPI (blue), Phalloidin (green), and anti-paxillin (red). Scale bar = 100 μm in all images, the stretch direction (B and H) was horizontal, represented by the black arrow, and white arrows (G and H) indicate focal adhesion sites randomly around the control cells and redistributed to the poles of stretched cells perpendicular to stretch. (For interpretation of the references to color in this figure legend, the reader is referred to the web version of this article).

Non-exposed photoresist was removed with SU8 developer (MicroChem). PDMS stamps (Sylgard 184 elastomer base with the curing agent 10:1, Dow–Corning, Midland, MI) were cured against the master and then removed, trimmed to size, and compressed against the STREX silicone elastic membranes. A corona was used to ionize the air to create a plasma around the electrode increasing the wettability of the substrate and PDMS, allowing a collagen type I fitc-conjugated solution (at a higher concentration 100 μg/mL overnight at 4 °C) solution to coat the surface through the microfabricated channels. Regions in contact with the PDMS did not have collagen type I and therefore did not promote cell attachment. The collagen was removed and the surface was rinsed and incubated with 3% BSA (in PBS) at 37 °C for 30 min. Cells were seeded on the membrane as described earlier, with the modification that after 30 min the cells remaining in the supernatant were removed and the surface was washed twice to ensure that only cells with good adhesion to the collagen remained. After 24 h the cells were stretched at 1 Hz, 20% strain for 24 h.

The small number of cells on the micropatterned membranes required apoptotic cells to be quantified using immunohistochemistry for cleaved caspase-3, a marker of apoptosis [23]. Cells were incubated with 10% neutral buffered formalin (30 min) and a 10% normal goat block (Vector Laboratories, Burlingame, CA, in 1% BSA/PBS, 30 min) and incubated overnight with a cleaved caspase-3 primary antibody (AB3623, Millipore, Temecula, CA, 1:250 in 1% BSA/PBS). The cells were stained with a goat anti-rabbit Alexa 546-conjugated secondary antibody (Invitrogen, 1/800), DAPI (1:1000), and Alexa 488-phalloidin (1/100). At least 20 cells were imaged for each chamber condition and percent apoptotic cells was calculated [positive caspase-3 staining/total cells × 100].

2.4. Statistics

All data was assessed for normality using the Ryan–Joiner test. A one-way ANOVA was done for flow cytometry, orientation results, and cleaved caspase-3 counts with a Fisher's post hoc test. A one sample *t*-test was done on the $\Delta\Delta C_T$ values to assess if there were any differences from control for each strain amplitude ($\Delta\Delta C_T = 0$). All statistics were done with Minitab software (Version 16, State College, PA) and significance was always defined as $p < 0.05$.

3. Results

Cell stretch on uniform collagen substrates resulted in a small trend of increased early stage apoptosis (Annexin V positive cells) in the detached cell population (affecting <1% of the cells) that was not significant (Supplementary 1A and B). No differences were observed for late stage apoptosis/necrosis (dual Annexin V and PI positive cells). CTS had variable effects on mRNA expression, with no significant changes (Supplementary 1C). The largest effect of stretching on uniformly coated collagen substrates was cellular reorientation (Fig. 2). Unstretched cells exhibited a random pattern of cellular orientations as quantified with DFT and autocorrelation (cross-correlation of a signal with itself), while all of the stretched cells had a preferential orientation that exhibited a Gaussian pattern. The mean of the Gaussian curve fit quantified maximum angle of alignment (where angles ranged from 0 to 180 degrees from the direction of stretch) and standard deviation indicated relative variance within the image. No significant differences in orientation were detected between stretch groups for both the mean (10%:86.4 ± 5.8°, 15%:102.0 ± 12.4°, 20%:86.0 ± 15.9°, $p = 0.274$) and standard deviation of the Gaussian curve fit (10%:67.6 ± 19.4°, 15%:47.2 ± 19.0°, 20%:128.4 ± 129.3°, one way ANOVA, $p = 0.273$). Cellular reorientation in response to stretch was associated with a clear redistribution of actin stress fibers (Phalloidin), and focal adhesion sites (Paxillin) perpendicular to the direction of stretch and some nuclear (DAPI) reorientation. Therefore, when cells were allowed to reorient little apoptosis and changes in gene expression occurred.

Cleaved caspase-3 staining on uniformly coated chambers was minimal for control and stretched cells (<8%, Fig. 3), supporting the flow cytometry results. There was also little observed cleaved caspase-3 staining (<5%) when the cells were grown without stretch on stripes of collagen that prevented reorientation. Stretching the cells on the striped substrate, however, resulted in a significant increase in percentage of cells positive for cleaved caspase-3

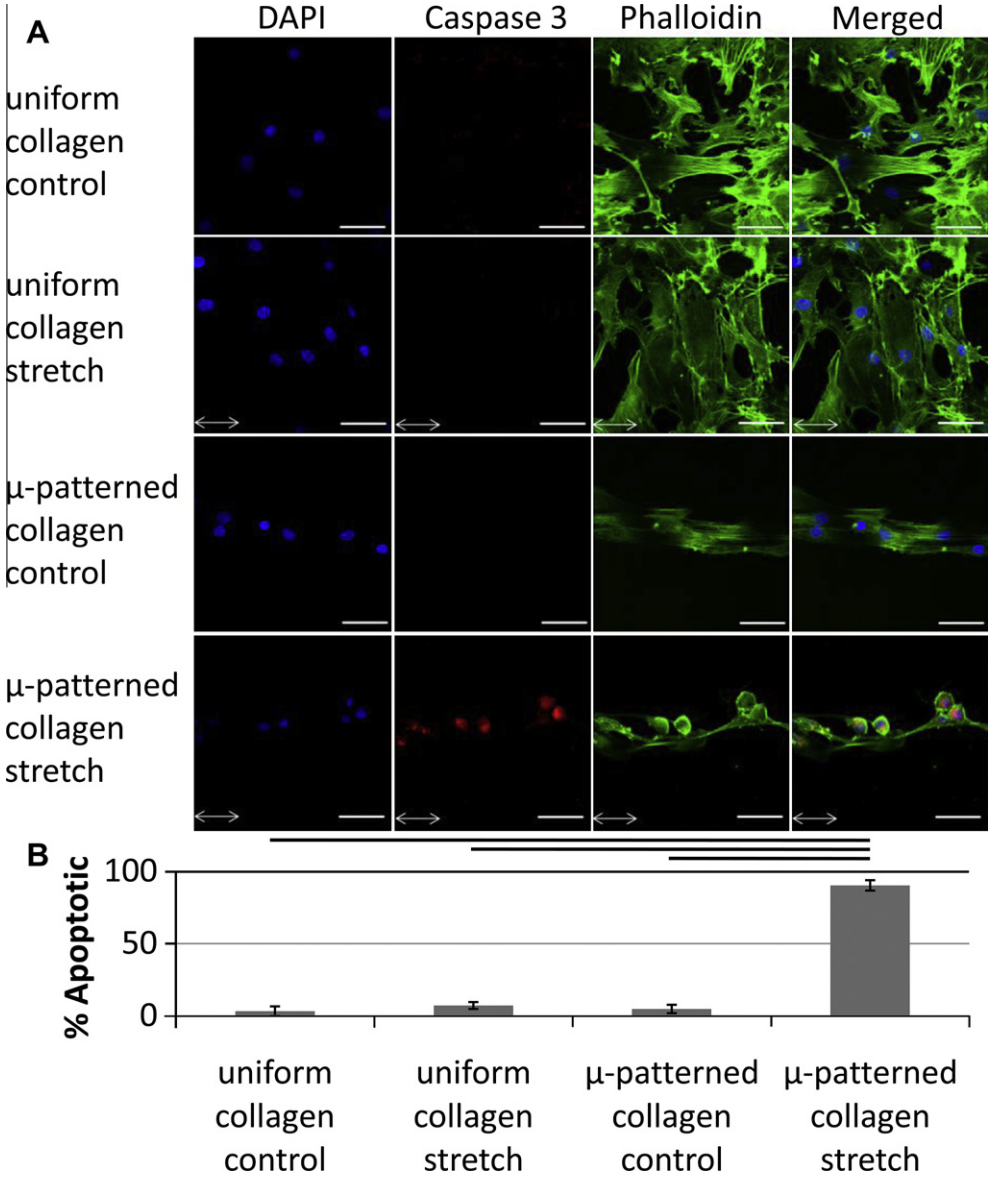

Fig. 3. Restricting the adaptive reorientation mechanism, and applying 20% cyclic stretch results in positive staining of cleaved caspase-3, indicating the initiation of an apoptotic pathway. Images of control and stretched cells on either a uniformly collagen coated substrate or restricted to 40 μm collagen stripes stained with DAPI (blue), cleaved caspase-3 (red), and Phalloidin (green) (A). The stretch direction was horizontal and is represented by a white arrow on the images. Scale bars are 50 μm. There was significantly more cleaved caspase-3 staining in the restricted orientation group subjected to 20% cyclic stretch (B, one way ANOVA, $p < 0.001$, Fisher's post hoc test) (For interpretation of the references to color in this figure legend, the reader is referred to the web version of this article).

(at least 20 cells for each group, one way ANOVA, $p < 0.001$, average of 90%). The restricted stretched cells also had an observed rounded, or 'blebbed' morphology.

4. Discussion

AF cells from surgical samples underwent cyclic uniaxial stretch to test the hypothesis that AF cells are capable of reorienting in response to high stretch magnitudes but undergo apoptosis when their adaptive reorientation is restricted. Results indicated that AF cells responded to 24 h of cyclic stretch on uniformly coated collagen surfaces by redistribution of actin and focal adhesions perpendicular to the stretch direction without notable apoptosis or matrix gene expression. However, AF cells were highly susceptible to stretch-induced apoptosis when adaptive reorientation was inhibited by restricting cell adhesion surfaces to 40 μm stripes parallel to the direction of stretch. Results support the concept that cells must maintain their ability to reorient in order to adapt to high strain environments. Specifically, degenerated AF cells have the capacity to reorient, but stretch-induced apoptosis may be a contributor to cell death during degeneration due to high strains concentrated around delaminations, herniations and other structural defects, since cells would have a reduced capacity to adapt in the more highly crosslinked, fibrotic, and compacted degenerated AF tissue.

Uniaxial cyclic stretching of 2D cell cultures causes the actin cytoskeleton and focal adhesions of many cell types to align perpendicular to the direction of stretch [15–17]. Different cell types orient at different rates, for instance, fibroblasts orient within 3 h [24] and vascular endothelial cells orient within 6 h [25], while some cell types, including neutrophils, do not reorient [26]. Reorientation perpendicular to direction of stretch is a mechanism for both remodeling and intracellular signaling by a structural and

biochemical adaption to mechanical stretch [27] related to Rho activity and the extent of cell stretching [17] that can be predicted by minimizing the potential energy of the stress fiber-focal adhesion complex [28]. All three strain amplitudes (10%, 15%, and 20%) in this study had similar effects on human AF cells and resulted in the same reorientation patterns. It is likely that minimizing the potential energy by cytoskeletal remodeling is an important adaptation that allows cells to adapt to high strains observed when collagen fibers undergo tension as occurs in bending and torsion in the IVD [29]. However, age and degeneration related changes in the collagen network, including increases in crosslink density [30,31], AF matrix remodeling [3], tissue compaction [32], and compromised lamellar structure [33] may limit the capacity for cells to reorient in response to high strains.

When cells were restricted from reorienting cleaved caspase-3 staining and a rounded cell morphology, often called "blebs" was observed. Cleavage of the effector protein, caspase-3 is critical for dismantling of the cell and the development of apoptotic bodies [23], while the "bleb" morphology is a result of the cell detaching from the underlying substrate as it undergoes apoptosis [34]. Therefore the restricted orientation model is consistent with the stretch-induced apoptosis observed in other studies on AF cells [12–14]. We highlight that differences in applied mechanical stimuli (uniaxial *vs.* biaxial) strongly influence cellular adaptive mechanisms. Excessive biaxial stretch leads to apoptosis [12–14] and in this study excessive uniaxial stretch leads to reorientation. However, when cells are unable to reorient to minimize strain energy (i.e., equibiaxial strain and/or uniaxial strain with restricted adhesion area) they are susceptible to apoptosis at high stretch magnitudes.

This *in vitro* model has the advantage of precise boundary conditions, to analyze the effect of stretch without confounding factors present in the more complex *in situ* environment, however, direct interpolation to the native environment is speculative. For example, pure tensile uniaxial strain will not always occur *in situ* [35]. Under healthy conditions AF surface strains up to 6% were measured along the fiber direction [10], therefore the strains chosen are high and are likely to only be present in degenerated states near structural defects, and injury sites. While these differences exist, we believe the inferences remain that cells with restricted motility are at greater risk of apoptosis. Finally, the cells used were obtained from degenerated human IVDs, which have an altered gene expression pattern compared to cells obtained from healthy IVDs [36]. However, it is likely that healthy AF cells are able to reorient in response to stretch since degenerated cells did.

In conclusions, high uniaxial strains on a uniformly coated collagen surface promoted cytoskeletal reorientation without apoptosis and with minimal alterations in gene expression. However, AF cells were vulnerable to stretch-induced apoptosis when cellular reorientation was restricted. Results indicate that degenerated AF cells have the capacity to adapt to stretch but that high strains and inhibited cellular reorientation, as might occur during degeneration, puts cells at risk of stretch-induced apoptosis. These AF cells exemplify, on a cellular-level, the famous quote of John Stark "Live free or die!"

Acknowledgments

This work made possible by funding from the NIH (R01AR051146, R01AR057397) and by the AO Research Fund (project F-09-10I) of the AO Foundation.

Appendix A. Supplementary data

Supplementary data associated with this article can be found, in the online version, at http://dx.doi.org/10.1016/j.bbrc.2012.04.018.

References

[1] S.R. Bibby, J.P. Urban, Effect of nutrient deprivation on the viability of intervertebral disc cells, Eur. Spine J. 13 (2004) 695–701.
[2] S.R. Bibby, D.A. Jones, R.M. Ripley, J.P. Urban, Metabolism of the intervertebral disc: effects of low levels of oxygen, glucose, and pH on rates of energy metabolism of bovine nucleus pulposus cells, Spine 30 (2005) 487–496.
[3] P.J. Roughley, Biology of intervertebral disc aging and degeneration: involvement of the extracellular matrix, Spine 29 (2004) 2691–2699.
[4] M.A. Adams, P.J. Roughley, What is intervertebral disc degeneration and what causes it? Spine 31 (2006) 2151–2161.
[5] G.D. O'Connell, E.J. Vresilovic, D.M. Elliott, Human intervertebral disc internal strain in compression: the effect of disc region, loading position, and degeneration, J. Orthop. Res. 29 (2011) 547–555.
[6] A. Tsantrizos, K. Ito, M. Aebi, T. Steffen, Internal strains in healthy and degenerated lumbar intervertebral discs, Spine 30 (2005) 2129–2137.
[7] G.D. O'Connell, N.R. Malhotra, E.J. Vresilovic, D.M. Elliott, The effect of discectomy and the dependence on degeneration of human intervertebral disc strain in axial compression, Spine 36 (2011) 1765–1771.
[8] A.J. Michalek, M.R. Buckley, L.J. Bonassar, I. Cohen, J.C. Iatridis, The effects of needle puncture injury on microscale shear strain in the intervertebral disc annulus fibrosus, Spine J. 10 (2010) 1098–1105.
[9] C.L. Korecki, J.J. Costi, J.C. Iatridis, Needle puncture injury affects intervertebral disc mechanics and biology in an organ culture model, Spine 33 (2008) 235–241.
[10] I.A. Stokes, Surface strain on human intervertebral discs, J. Orthop. Res. 5 (1987) 348–355.
[11] K.B. Broberg, On the mechanical behaviour of intervertebral discs, Spine 8 (1983) 151–165.
[12] F. Rannou, T.S. Lee, R.H. Zhou, J. Chin, J.C. Lotz, M.A. Mayoux-Benhamou, J.P. Barbet, A. Chevrot, J.Y. Shyy, Intervertebral disc degeneration: the role of the mitochondrial pathway in annulus fibrosus cell apoptosis induced by overload, Am. J. Pathol. 164 (2004) 915–924.
[13] Y.H. Zhang, C.Q. Zhao, L.S. Jiang, L.Y. Dai, Cyclic stretch-induced apoptosis in rat annulus fibrosus cells is mediated in part by endoplasmic reticulum stress through nitric oxide production, Eur. Spine J. 20 (2011) 1233–1243.
[14] Y.H. Zhang, C.Q. Zhao, L.S. Jiang, L.Y. Dai, Lentiviral shRNA silencing of CHOP inhibits apoptosis induced by cyclic stretch in rat annular cells and attenuates disc degeneration in the rats, Apoptosis 16 (2011) 594–605.
[15] A.C. Ritchie, S. Wijaya, W.F. Ong, S.P. Zhong, K.S. Chian, Dependence of alignment direction on magnitude of strain in esophageal smooth muscle cells, Biotechnol. Bioeng. 102 (2009) 1703–1711.
[16] F. Boccafoschi, M. Bosetti, S. Gatti, M. Cannas, Dynamic fibroblast cultures: response to mechanical stretching, Cell Adh. Migr. 1 (2007) 124–128.
[17] R. Kaunas, P. Nguyen, S. Usami, S. Chien, Cooperative effects of Rho and mechanical stretch on stress fiber organization, Proc. Natl. Acad. Sci. U. S. A. 102 (2005) 15895–15900.
[18] J.P. Thompson, R.H. Pearce, M.T. Schechter, M.E. Adams, I.K. Tsang, P.B. Bishop, Preliminary evaluation of a scheme for grading the gross morphology of the human intervertebral disc, Spine 15 (1990) 411–415.
[19] P. Waring, D. Lambert, A. Sjaarda, A. Hurne, J. Beaver, Increased cell surface exposure of phosphatidylserine on propidium iodide negative thymocytes undergoing death by necrosis, Cell Death Differ. 6 (1999) 624–637.
[20] J.P. Marquez, Fourier analysis and automated measurement of cell and fiber angular orientation distributions, Int. J. Solids Struct. 43 (2006) 6413–6423.
[21] N.V. Swindale, Orientation tuning curves: empirical description and estimation of parameters, Biol. Cybern. 78 (1998) 45–56.
[22] E. Kim, Y. Xia, G.M. Whitesides, Micromolding in capillaries: applications in materials science, J. Am. Chem. Soc. 118 (1996) 5722–5731.
[23] A.G. Porter, R.U. Janicke, Emerging roles of caspase-3 in apoptosis, Cell Death Differ. 6 (1999) 99–104.
[24] C. Neidlinger-Wilke, E. Grood, L. Claes, R. Brand, Fibroblast orientation to stretch begins within three hours, J. Orthop. Res. 20 (2002) 953–956.
[25] T. Iba, B.E. Sumpio, Morphological response of human endothelial cells subjected to cyclic strain in vitro, Microvasc. Res. 42 (1991) 245–254.
[26] W.S. Haston, J.M. Shields, P.C. Wilkinson, The orientation of fibroblasts and neutrophils on elastic substrata, Exp. Cell Res. 146 (1983) 117–126.
[27] R. Kaunas, S. Usami, S. Chien, Regulation of stretch-induced JNK activation by stress fiber orientation, Cell Signal 18 (2006) 1924–1931.
[28] D. Stamenovic, K.A. Lazopoulos, A. Pirentis, B. Suki, Mechanical stability determines stress fiber and focal adhesion orientation, Cell Mol. Bioeng. 2 (2009) 475–485.
[29] M. Krismer, C. Haid, W. Rabl, The contribution of anulus fibers to torque resistance, Spine 21 (1996) 2551–2557.
[30] S.S. Sivan, E. Tsitron, E. Wachtel, P. Roughley, N. Sakkee, F. van der Ham, J. Degroot, A. Maroudas, Age-related accumulation of pentosidine in aggrecan and collagen from normal and degenerate human intervertebral discs, Biochem. J. 399 (2006) 29–35.
[31] H.K. Pokharna, F.M. Phillips, Collagen crosslinks in human lumbar intervertebral disc aging, Spine 23 (1998) 1645–1648.
[32] J.C. Iatridis, L.A. Setton, R.J. Foster, B.A. Rawlins, M. Weidenbaum, V.C. Mow, Degeneration affects the anisotropic and nonlinear behaviors of human anulus fibrosus in compression, J. Biomech. 31 (1998) 535–544.
[33] S. Bernick, J.M. Walker, W.J. Paule, Age changes to the anulus fibrosus in human intervertebral discs, Spine 16 (1991) 520–524.

[34] Q. Lu, S. Rounds, Focal adhesion kinase and endothelial cell apoptosis, Microvasc. Res. (2011).
[35] S.B. Bruehlmann, J.R. Matyas, N.A. Duncan, ISSLS prize winner: collagen fibril sliding governs cell mechanics in the anulus fibrosus: an in situ confocal microscopy study of bovine discs, Spine 29 (2004) 2612–2620.
[36] H.E. Gruber, G.L. Hoelscher, E.N. Hanley Jr, Annulus cells from more degenerated human discs show modified gene expression in 3D culture compared with expression in cells from healthier discs, Spine J. 10 (2010) 721–727.